Re-submitted to: *Chemosphere* (CHEM 22722, revised as a Technical Note)

Date: 19 August 2011

Investigation of the role of biopolymer clusters in MBR membrane fouling using flash freezing and environmental scanning electron microscopy

Xiao-mao Wang,[a] Fei-yun Sun[a,b] and Xiao-yan Li[a]*

[a] Environmental Engineering Research Centre, Department of Civil Engineering, The University of Hong Kong, Pokfulam Road, Hong Kong, China

[b] Harbin Institute of Technology, Shenzhen Graduate School, Shenzhen 518055, China

(*Corresponding author: phone: 852-28592659; fax: 852-28595337; email: xlia@hkucc.hku.hk)

Abstract

The technique that employs flash freezing and environmental scanning electron microscopy (ESEM) was utilised for detailed investigation of the fouling materials in a membrane bioreactor (MBR). The method involves the flash freezing of a wet sample in liquid nitrogen for 10 s to preserve its structure for direct ESEM observation with a high image resolution. ESEM images show that the sludge cake formed by simple filtration of the MBR bulk sludge has a highly porous, sponge-like structure with a fairly low resistance. However, the fouling layer attached to the membrane surface contains a thin gel-layer under the main body of the sponge-like sludge cake, which is similar to that formed by filtration of a dispersion of biopolymer clusters (BPCs). It is apparent that BPCs tend to accumulate on the membrane surface, and the gel layer is largely responsible for the high filtration resistance of the cake layer on the fouled membranes.

Keywords: Biological wastewater treatment; Biopolymer clusters (BPCs); Environmental scanning electron microscope (ESEM); Flash freezing; Fouling layer; Membrane bioreactor (MBR).

1. Introduction

Membrane bioreactors (MBRs) are increasingly applied to biological wastewater treatment owing to their ensured solids–water separation and excellent effluent quality for reuse purposes (Judd, 2006; Yang et al., 2006). However, membrane fouling, which is caused primarily by foulant deposition on the membrane surface, remains far and away the major limitation to the cost-effectiveness of MBRs for large-scale applications (Asatekin et al., 2007). Numerous efforts have been devoted to obtaining a fundamental understanding of the membrane fouling mechanisms (Le-Clech et al., 2006) that is essential for the development of effective fouling control technologies. It is generally believed that the deposition of a fouling (cake or gel) layer on the membrane surface is the major form of membrane fouling during MBR operation (Chu and Li, 2005; Wang et al., 2007). A number of foulants have been identified that would be responsible for the fouling layer formation, including biomass sludge (Defrance et al., 2000), the extracellular polymeric substances (EPS) in sludge (Nagaoka et al., 1996; Drews et al., 2006), soluble microbial products (SMP) and other forms of organic matter in the liquid phase (Rosenberger et al., 2006; Liang et al., 2007). Therefore, the roles played by different foulants, and their interactions in membrane fouling during MBR operation, however, still require investigation.

The supernatant of the MBR sludge mixture has been found to have a consistently higher organic concentration than the effluent from the MBR (Shin and Kang, 2003; Holakoo et al., 2006). It is therefore believed that the organic materials in the sludge suspension

contribute significantly to the development of membrane fouling (Judd, 2006; Ng et al., 2006; Rosenberger et al., 2006; Liang et al., 2007). Studies have further indicated that biopolymer clusters (BPCs) are one of the primary foulants in the MBR system (Wang et al., 2007; Sun et al., 2008; Wang and Li, 2008). BPCs are formed by the clustering of SMP and loose EPS in the sludge cake. BPCs are much larger in size than SMP, and they differ from bacterial flocs in that they are composed of few microorganisms. It has become clear that the difference in organic concentration between the supernatant of the MBR sludge and its permeate effluent is due to the retention of BPCs by membrane filtration. Meanwhile, BPC formation and accumulation in turn would cause serious membrane fouling during MBR operation (Sun et al., 2010b). However, the role played by BPCs in fouling layer formation and its effect on membrane permeability remain to be determined.

Detailed examination of the fouling layer structure on the membrane surface is greatly needed for better understanding of the MBR fouling mechanisms and the interactions of different foulants during the fouling process. Such examination is also extremely important to the development of more effective membrane fouling alleviation strategies. For example, a further increase in shear intensity may not be effective for membrane fouling reduction if the top layers of the sludge cake contribute little to its filtration resistance. Similarly, the commonly applied back-flushing technique (Wu et al., 2008) may have a low degree of effectiveness if BPCs accumulate mainly at the bottom of the sludge cake and cover the membrane surface. Chemical cleaning from the permeate side may be more effective in this case (Chang et al., 2002). The advanced microscopic techniques used to date to examine foulants and fouling layers, including scanning electron microscopy (SEM), confocal laser scanning microscopy (CLSM) and atomic force microscopy (AFM), are unsatisfactory. Conventional SEM examination requires samples to undergo dehydration followed by sputter coating (Miura et al., 2007), whereas samples for CLSM must be stained using specific

fluorescent dyes before observation (Chu and Li, 2005; Hwang et al., 2008). As the foulants are highly hydrated, porous and soft, the SEM sample pretreatment steps can cause the significant deformation, or even collapse, of the structure and morphology of the foulants and fouling layers (Fig. 1a and 1b). AFM scan requests little sample treatment and the images can have a fairly high resolution. This, however, is the case only for rather hard surfaces. The AFM images of the fouling layers on membrane are usually blurry owing to the soft nature of the foultants (Huisman et al., 2000; Martinez et al., 2000; Song et al., 2004). Moreover, AFM as a surface scanning technique is apparently not suitable for examination of thick sludge cake layers, as is also the case for CLSM. In the latter, the free dyes may remain in the cake, and the fouling layers may produce false images that are difficult to discern.

Environmental SEM (ESEM, or, more generally, variable-pressure SEM) is another technique employed for the direct observation of highly hydrated samples including fouling layers (Le-Clech et al., 2007), but requires no dehydration and sputter coating steps. Omission of the dehydration step allows preservation of the sample contents and structure. However, the maximum magnification possible for ESEM observations at room temperature could be restricted, being determined by the limitation of the useful specimen distance, which may lead to a loss of specimen details. Thus, most ESEM images of the fouling layers on the membrane surface look rather blurry (Le-Clech et al., 2007). The other problem for ESEM is the specimen dehydration resulted from water evaporation at room temperature in the low-pressure (one to several hundred Pa) specimen chamber, which often leads to significant sample shrinkage and structure deformation. This problem is more severe for highly hydrated specimens, as is the case for the gel and/or cake layers responsible for membrane fouling (Fig. 1c and 1d). However, both the magnification and resolution can be significantly improved and the specimen dehydration can be greatly minimized if the specimen is cryogenically

fixed and maintained frozen on the cold stage during ESEM examinations (Santiwong et al., 2009; Wang and Waite, 2009).

In this study, the flash freezing technique with liquid nitrogen coupled with ESEM examination was adopted for the first time to examine the shape and structure of the MBR foulants and fouling layers. In view of the known role of BPCs in membrane fouling, focuses were placed on the characterisation of the fouling properties of BPCs and determination of the spatial distribution of BPCs in the sludge cake layer. The findings would provide important insight into the mechanisms of membrane fouling in MBRs.

2. Materials and methods

2.1. Sludge and BPC samples

The sludge and BPC samples were obtained from a submerged MBR that had been in stable operation for more than 4 yr (Sun et al., 2010b). A 0.2 m^2 polyethylene hollow-fibre membrane module was immersed in the cuboid plexiglass reactor, which had a working volume of 5 L. The feed to the reactor was a mixture of synthetic wastewater and actual domestic sewage. The synthetic wastewater was prepared according to the basic recipe of AEESP (2001) to supply about 90% of the organic load in the influent, and the actual sewage was collected from a local wastewater treatment plant (Stanley Sewage Treatment Works, Hong Kong). The influent had a total organic carbon (TOC) concentration of around 220 mg L^{-1}, and the concentration of the mixed liquor suspended solids (MLSS) in the MBR was maintained at about 5.1 g L^{-1}. Continuous aeration was applied under the membrane module, and an intermittent filtration mode was applied with a switch on/off ratio of 18 min/2 min for membrane fouling minimisation. The sludge and hydraulic retention times were 20 d and 6 h, respectively, which corresponded to a food-to-microorganism ratio of 0.125 g TOC g^{-1} MLSS

125 d^{-1} and a filtration flux of 0.1 m^3 m^{-2} d^{-1}. The reactors were operated at room temperature (22-
126 25 ºC), and the water temperature was 20-22 ºC. The TOC concentration in the liquid
127 samples was determined with a TOC analyser (IL550 TOC-TN Analyzer, Lachat).

128 The bulk sludge (BS) was obtained directly from the MBR sludge mixture. Special
129 attention was paid to the cake sludge (CS) that gradually built up on the membrane during
130 MBR operation. When the membrane was severely fouled, as indicated by a trans-membrane
131 pressure (TMP) of about 80 kPa, the CS deposited on the membrane was thoroughly removed
132 from the membrane fibres and re-suspended in water until to a sludge concentration of about
133 5 g MLSS L^{-1}. In addition to the CS mixture, the CS suspension was further separated by
134 sedimentation at 4 ºC for 12 h into the CS supernatant and settled CS solids. The CS
135 supernatant is known to contain a high concentration of organic solutes deemed to be BPCs
136 (Wang et al., 2007; Lin et al., 2009). A filterability test was carried out on the four samples,
137 i.e., the BS mixture, CS suspension, settled CS solids and CS supernatant, to determine their
138 specific resistance to filtration. The filtration test was conducted using microfiltration (MF)
139 membrane filters (0.4 μm, Osmosis) following the method that has been used by Wisniewski
140 and Grasmick (1998) and Wang et al. (2007). More importantly, the sludge or gel layers
141 deposited on the MF filters were then processed for the subsequent ESEM examination.
142
143 *2.2. ESEM observation*

144 A flash freezing technique was adopted to preserve the sludge or gel layers. This
145 method has been previously employed (Santiwong et al., 2008; Wang and Waite, 2008) to
146 examine the structure of highly porous gel layers. As stated above, resolution of the ESEM
147 images can also be greatly enhanced if the wet samples are fixed by freezing. Prior to ESEM
148 observation, each membrane filter with a wet cake or gel layer was carefully cut into 10 × 5
149 mm slices. The filter with the sample was then dipped in a liquid nitrogen bath for about 10 s.

After the simple flash freezing, the sample was frozen into a fragile solid that could easily be snapped to display a nearly flat edge or cutaway section. The sample specimen was then placed under an ESEM (S-3400N, variable-pressure SEM, Hitachi) on a cold stage (-25 ºC, MK2-cool stage, Deben). The sample was not conductive, and a back-scattered electron (BSE) signal was used for imaging. In actuality, use of BSE signal is necessary to allow a high resolution of the ESEM images. Moreover, the fouled membrane fibres were also cut off from the MBR, and the morphology and micro-structure of the CS formed on the membrane surface were examined using the same flash freezing-ESEM technique.

3. Results and discussion

3.1 Sludge and BPC layers

The volume and structure of the wet sludge deposition on the filter surface were well preserved by the flash freezing method using liquid nitrogen, thus allowing the porous structure of the deposition layer to be examined directly via ESEM. A highly porous structure with many large pores (Fig. 2) was observed for the cake layer formed through filtration of the BS suspension from the MBR. The size of these pores was apparently of the same magnitude as the sludge flocs, i.e., tens of μm. The packing of the sludge flocs was found to form a sponge-like structure conducive to water passage. Such distinct ESEM images showing the micro-structural details of the sludge cake would not be obtained with the conventional SEM (Fig. 1a and 1b), which requires a dehydration step. In comparison to the ESEM photos of the sludge cake taken at room temperature without prior flash freezing (Fig. 1c and 1d), the quality of the images in Fig. 2 is largely improved in terms of both resolution and structure preservation.

Filtration of the MBR BS suspension through the MF filter was actually fairly easy. The filtration test showed the BS mixture to have a mass-based specific resistance of only 3.4 × 10^{11} m kg^{-1} (Fig. 3), which is comparable to that reported by Buyukkamaci (2004) and Wang et al. (2007). The degree of filtration resistance remained low when a thick BS cake layer was formed on the MF filter. It can thus be deduced that the membrane module in a MBR would not become seriously fouled if only such a sludge cake was formed on the membrane.

The CS mixture, in contrast, was rather difficult to filter through the MF filter. The CS removed from the fouled membrane in the MBR displayed a much greater specific filtration resistance, i.e., at a level of around 1.4 × 10^{14} m kg^{-1} (Fig. 3). The CS had a high organic content, about 20 mg TOC g^{-1} SS, much higher than that of the MBR BS, which was around 1 mg TOC g^{-1} SS. The settled CS solids underwent an order of magnitude reduction in specific filtration resistance (around 2.1 × 10^{12} m kg^{-1}) compared to the original CS mixture. The organic content of the CS was dissolved into the supernatant to give it a TOC concentration of more than 40 mg L^{-1}. The CS supernatant had a much lower filterability, as it formed a gel layer on the MF filter with a specific resistance (around 1.7 × 10^{14} m kg^{-1}) similar to that of the CS mixture. The organic solutes in the supernatant, which are classified as BPCs, have been recognised as an important foulant in MBR systems (Wang et al., 2007; Sun et al., 2008). BPCs play an essential role in sludge deposition and cake layer formation on the membrane surface during MBR operation, and they are also primarily responsible for the great filtration resistance of the CS (Wang and Li, 2008; Lin et al., 2009; Sun et al., 2011a, 2011b).

The flash freezing treatment allows direct examination of BPCs on the filter surface (Fig. 4). The BPC layer showed a gel appearance that is rather different from the BS observed in Fig. 3. Despite its great filtration resistance, the gel layer formed on the MF filter was only

a few μm in thickness. The dehydration step for common SEM observation would greatly change the nascent structure and volume of the BPC gel layer. In contrast, as no dehydration was involved in sample preparation, the BPC layer structure was preserved in the present study. BPCs are in nature microgels formed by the clustering of SMP, small BPCs and loose EPS (Wang et al., 2007; Sun et al., 2008). It is apparent that BPCs in the gel layer were inter-connected (gelated) probably with the aid of multivalent cations (Wang and Waite, 2009). As a result, the gel layer did not have a sponge-like porous structure. It instead had a very low porosity at the top surface, which would effectively restrict the passage of water through the gel layer. Moreover, it is rather difficult to dehydrate a gel, which would further account for the extremely high specific resistance of the gel layer.

3.2 Fouling cake layer on the MBR membrane surface

The sludge cake layer on the membrane surface has been investigated in previous studies. The influences of the operating parameters, such as filtration flux, organic loading and sludge age, on the MBR fouling process were studied through laboratory experiments (Wang and Li, 2008). The membrane fouling rate was found to be affected by both the process variables and the BPC concentration in the sludge mixture. The specific filtration resistance of the cake layer correlated well with the BPC content in the sludge cake (Wang et al., 2007). In other words, BPC accumulation appeared to be the primary reason for the high specific resistance of the sludge fouling layer in MBRs. Because a high hydraulic shear is normally applied for membrane fouling control during MBR operation, massive sludge deposition on the membrane is usually prevented if the filtration is below the critical flux (Cho and Fane, 2002). However, an elevated shear intensity and a lower filtration flux would favour BPC accumulation in the sludge cake (Wang et al., 2007).

223 The structural detail of the cake sludge formed on the membrane fibre in the MBR
224 was also revealed by the ESEM images (Fig. 5a and 5b). When the membrane module was
225 severely fouled, the CS layer could be over 200 μm thick and sometimes cover more than one
226 fibre. The CS layer attached to the membrane was different from the BS deposition formed
227 during the filtration test, as indicated by the specific resistance of the former two orders
228 magnitude higher than that of the latter (Fig. 3). The principal morphology of the CS fouling
229 layer was similar to that of the BS deposition in terms of the porous structure (porosity and
230 pore size). However, by a scrutiny of the ESEM images one can find that at the bottom of the
231 CS layer there was a thin (several μm) layer that had a reticulum-like appearance with a mesh
232 of nodules. The above sponge-like main body formed by biomass sludge could be easily
233 detached while the thin layer remained attached to the membrane (Fig. 5c and 5d). The thin
234 layer was composed mainly of organic substances and apparently similar to the BPC gel layer
235 shown in Fig. 4.
236 The ESEM images also showed the BPC distribution within the CS layer to be non-
237 uniform, with the BPCs prone to accumulate at the bottom. Compared to CLSM images (Chu
238 and Li, 2005; Hwang et al., 2008), ESEM images have a higher resolution and show
239 structural details more clearly. The strong filtration resistance exhibited by the CS is likely
240 owing to the thin BPC layer, as the top sponge-like structure is fairly permeable. As organic
241 solutes, BPCs are sticky and flexible and can penetrate with water through the main body of
242 the porous sludge cake. Over the course of time, however, BPCs would become too large to
243 pass through the membrane, which could result in their accumulation and thus the formation
244 of a gel layer on the membrane surface. A small amount of BPC deposition on the membrane
245 would be sufficient to greatly increase its filtration resistance.
246 It is therefore apparent that BPC coverage of the membrane was brought about
247 primarily by the retention of organic materials such as SMP during MBR filtration. The

accumulation of BPCs in the sludge cake layer would also allow the BPCs to grow in size. The size of the BPCs in sludge cake has been found to be significantly larger than that in MBR sludge suspension (Sun et al., 2011b). During MBR operation, in which hydraulic shear is commonly applied, the BPCs that have not reached the membrane surface, but bind with the sludge flocs, have a strong chance of being scoured back into the bulk suspension. Thus, the formation of the thin BPC gel layer on the MBR membrane surface was the result of long-term operation (e.g., several weeks). Both the ESEM images and the filtration test showed a thin BPC layer to be sufficient to cause severe membrane fouling. BPC formation and accumulation within the CS layer are inevitable consequences of the inherent feature of membrane filtration during MBR operation, i.e., the retention of biomass sludge and organic foulants, thereby leading to membrane fouling.

4. Conclusions

An effective flash freezing-ESEM technique for investigation of fouling layers has been developed. ESEM images showed the sludge cake formed by simple filtration of the BS to be highly porous and permeable with a sponge-like structure. Filtration of the BPC dispersion, however, led to the formation of a gel-layer that was less porous, much less permeable and displayed a reticulum-like appearance. The CS layer formed was found to contain a thin (< 10 μm) gel-layer under the main body of the sponge-like sludge cake, which is largely responsible for the great specific filtration resistance of the cake layer.

Acknowledgments

This research was supported by URC funding from the University of Hong Kong, Special Equipment Grant SEG_HKU10 from the University Grants Committee (UGC), and Grants HKU7144/E07 and HKU714811E from the Research Grants Council (RGC) of the

Hong Kong SAR Government. The technical assistance of Mr. Keith C. H. Wong is greatly appreciated.

References

AEESP, 2001. Environmental Engineering Process Laboratory Manual. Association of Environmental Engineering and Science Professors, Champaign, IL, USA.

Asatekin, A., Kang, S., Elimelech, M., Mayes, A.M., 2007. Anti-fouling ultrafiltration membranes containing polyacrylonitrile-graft-poly (ethylene oxide) comb copolymer additives. J. Membr. Sci. 298, 136–146.

Buyukkamaci, N., 2004. Biological sludge conditioning by Fenton's reagent. Process Biochem. 39, 1503–1506.

Chang, I.S., Le-Clech, P., Jefferson, B., Judd, S., 2002. Membrane fouling in membrane bioreactors for wastewater treatment. J. Environ. Eng.-ASCE. 128, 1018–1029.

Cho, B.D., Fane, A.G., 2002. Fouling transients in nominally sub-critical flux operation of a membrane bioreactor. J. Membr. Sci. 209, 391–403.

Chu, H.P., Li, X.Y., 2005. Membrane fouling in a membrane bioreactor (MBR): Sludge cake formation and fouling characteristics. Biotechnol. Bioeng. 90, 323–331.

Defrance, L., Jaffrin, M.Y., Gupta, B., Paullier, P., Geaugey, V., 2000. Contribution of various constituents of activated sludge to membrane bioreactor fouling. Bioresour. Technol. 73, 105–112.

Drews, A., Lee, C.H., Kraume, M., 2006. Membrane fouling – a review on the role of EPS. Desalination 200, 186–188.

Holakoo, L., Nakhla, G., Yanful, E.K., Bassi, A.S., 2006. Chelating properties and molecular weight distribution of soluble microbial products from an aerobic membrane bioreactor. Water Res. 40, 1531–1538.

298 Huisman, I.H., Pradanos, P., Hernandez, A., 2000. The effect of protein-protein and protein-
299 membrane interactions on membrane fouling in ultrafiltration. J. Membr. Sci. 179, 79–
300 90.
301 Hwang, B.K., Lee, W.N., Yeon, K.M., Park, P.K., Lee, C.H., Chang, I.S., Drews, A., Kraume,
302 M., 2008. Correlating TMP increases with microbial characteristics in the bio-cake on
303 the membrane surface in a membrane bioreactor. Environ. Sci. Technol. 42, 3963–3968.
304 Judd, S., 2006. The MBR Book: Principles and Applications of Membrane Bioreactors in
305 Water and Wastewater Treatment. Elsevier, Amsterdam, The Netherlands.
306 Le-Clech, P., Chen, V., Fane, T.A.G., 2006. Fouling in membrane bioreactors used in
307 wastewater treatment. J. Membr. Sci. 284, 17–53.
308 Le-Clech, P., Marselina, Y., Ye, Y., Stuetz, R.A., Chen, V., 2007. Visualisation of
309 polysaccharide fouling on microporous membrane using different characterisation
310 techniques. J. Membr. Sci. 290, 36–45.
311 Liang, S., Liu, C., Song, L., 2007. Soluble microbial products in membrane bioreactor
312 operation: behaviors, characteristics, and fouling potential. Water Res. 41, 95–101.
313 Lin, H.J., Xie, K., Mahendran, B., Bagley, D.M., Leung, K.T., Liss, S.N., Liao, B.Q., 2009.
314 Sludge properties and their effects on membrane fouling in submerged anaerobic
315 membrane bioreactors (SAnMBRs), Water Res. 43, 3827–3837.
316 Martinez, F., Martin, A., Pradanos, P., Calvo, J.I., Palacio, L., Hernandez, A., 2000. Protein
317 adsorption and deposition onto microfiltration membranes: The role of solute-solid
318 interactions. J. Colloid Interface Sci. 221, 254–261.
319 Miura, Y., Watanbe, Y., Okabe, S., 2007. Membrane biofouling in pilot-scale membrane
320 bioreactors (MBRs) treating municipal wastewater: impact of biofilm formation.
321 Environ. Sci. Technol. 41, 632–638.

322 Nagaoka, H., Ueda, S., Miya, A., 1996. Influence of bacterial extracellular polymers on the
323 membrane separation activated sludge process. Water Sci. Technol. 34(9), 165–172.
324 Ng, H.Y., Tan, T.W., Ong, S.L., 2006. Membrane fouling of submerged membrane
325 bioreactors: Impact of mean cell residence time and the contributing factors. Environ.
326 Sci. Technol. 40, 2706–2713.
327 Rosenberger, S., Laabs, C., Lesjean, B., 2006. Impact of colloidal and soluble organic
328 material on membrane performance in membrane bioreactors for municipal wastewater
329 treatment. Water Res. 40, 710–720.
330 Santiwong, S.R., Guan, J., Waite, T.D., 2008. Effect of ionic strength and pH on hydraulic
331 properties and structure of accumulating solid assemblages during microfiltration of
332 montmorillonite suspensions. J. Colloid Interface Sci. 317, 214–227.
333 Shin, H.S., Kang, S.T., 2003. Characteristics and fates of soluble microbial products in
334 ceramic membrane bioreactor at various sludge retention times. Water Res. 37, 121–127.
335 Song, W., Ravindran, V., Koel, B.E., Pirbazari, M., 2004. Nanofiltration of natural organic
336 matter with H_2O_2/UV pretreatment: fouling mitigation and membrane surface
337 characterization. J. Membr. Sci. 241, 143–160.
338 Sun, F.Y., Wang, X.M., Li, X.Y., 2008. Visualisation and characterisation of biopolymer
339 clusters in a submerged membrane bioreactor. J. Membr. Sci. 325, 691–697.
340 Sun, F.Y., Wang, X.M., Li, X.Y., 2011a. Effect of biopolymer clusters on the fouling
341 property of sludge from a membrane bioreactor (MBR) and its control by ozonation.
342 Process Biochem. 46, 162–167.
343 Sun, F.Y., Wang, X.M., Li, X.Y., 2011b. Change in the fouling propensity of sludge in
344 membrane bioreactors (MBR) in relation to the accumulation of biopolymer clusters.
345 Bioresour. Technol. 102, 4718–4725.

346 Wang, X.M., Li, X.Y., 2008. Accumulation of biopolymer clusters in a submerged membrane
347 bioreactor and its effect on membrane fouling. Water Res. 42, 855–862.
348 Wang, X.M., Li, X.Y., Huang, X., 2007. Membrane fouling in a submerged membrane
349 bioreactor (SMBR): Characterisation of the sludge cake and its high filtration resistance.
350 Sep. Purif. Technol. 52, 439–445.
351 Wang, X.M., Waite, T.D., 2008. Impact of gel layer formation on colloid retention in
352 membrane filtration processes. J. Membr. Sci. 325, 486–494.
353 Wang, X.M., Waite, T.D., 2009. Role of gelling soluble and colloidal microbial products in
354 membrane fouling. Environ. Sci. Technol. 43, 9341–9347.
355 Wisniewski, C., Grasmick, A., 1998. Floc size distribution in a membrane bioreactor and
356 consequences for membrane fouling. Colloids Surf. A 138, 403–411.
357 Wu, J., Le-Clech, P., Stuetz, R.M., Fane, A.G., Chen, V., 2008. Effect of relaxation and
358 backwashing conditions on fouling in membrane bioreactor. J. Membr. Sci. 324, 26–32.
359 Yang, W.B., Cicek, N., Ilg, J., 2006. State-of-the-art of membrane bioreactors: worldwide
360 research and commercial applications in North America. J. Membr. Sci. 270, 201–211.
361
362

363 **Figure Captions**

364

365 Fig 1. Micrographs of the activated sludge cake layer obtained (a, b) with a conventional
366 SEM after sample pretreatment involving dehydration and sputter coating and (c, d) with
367 an ESEM at room temperature without prior flash freezing. The arrow points to the
368 membrane filter.

369 Fig. 2. ESEM images of (a) the cross-section and (b, c, d) detailed structure of the sludge
370 cake formed on a MF membrane filter through direct filtration of the suspended bulk
371 sludge in a MBR. The arrows point to the membrane filter.

372 Fig. 3. Comparison of the specific filtration resistance of the cake and gel layers formed
373 during filtration of the MBR bulk sludge (AS mixture), the re-suspended MBR cake
374 sludge (CS mixture), the settled solids of the CS mixture and the CS supernatant after
375 settling.

376 Fig. 4. ESEM images of a layer of BPCs retained on the MF membrane filter through
377 filtration of BPC dispersion, with increasing magnification from (a) to (d). The arrows
378 point to the membrane filter.

379 Fig. 5. ESEM images of (a, b) the sludge cake layer deposited on the membrane module in
380 the MBR and (c, d) its bottom BPC layer after removal of the main body of the sludge
381 cake. The arrows point to the hollow-fibre membrane.

382

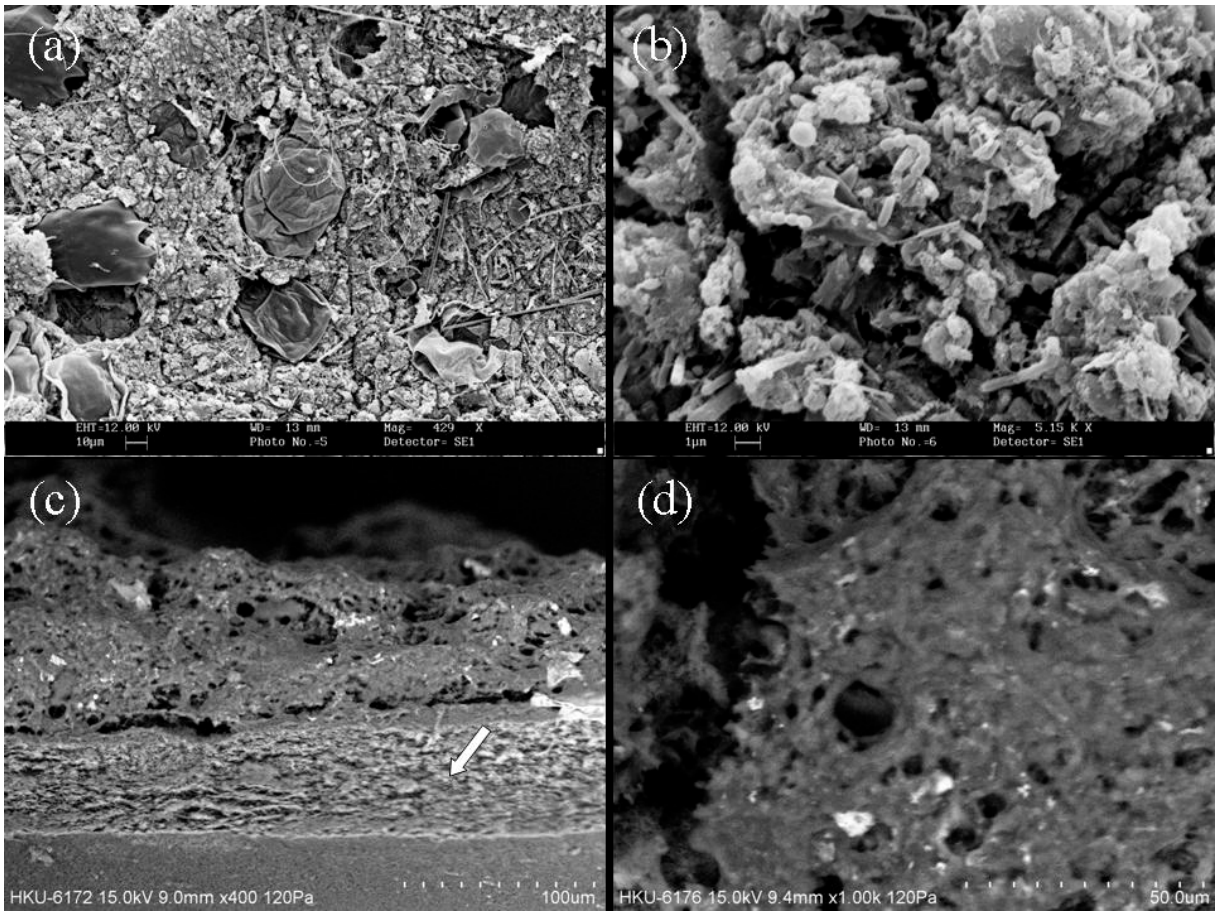

Fig 1. Micrographs of the activated sludge cake layer obtained (a, b) with a conventional SEM after sample pretreatment involving dehydration and sputter coating and (c, d) with an ESEM at room temperature without prior flash freezing. The arrow points to the membrane filter.

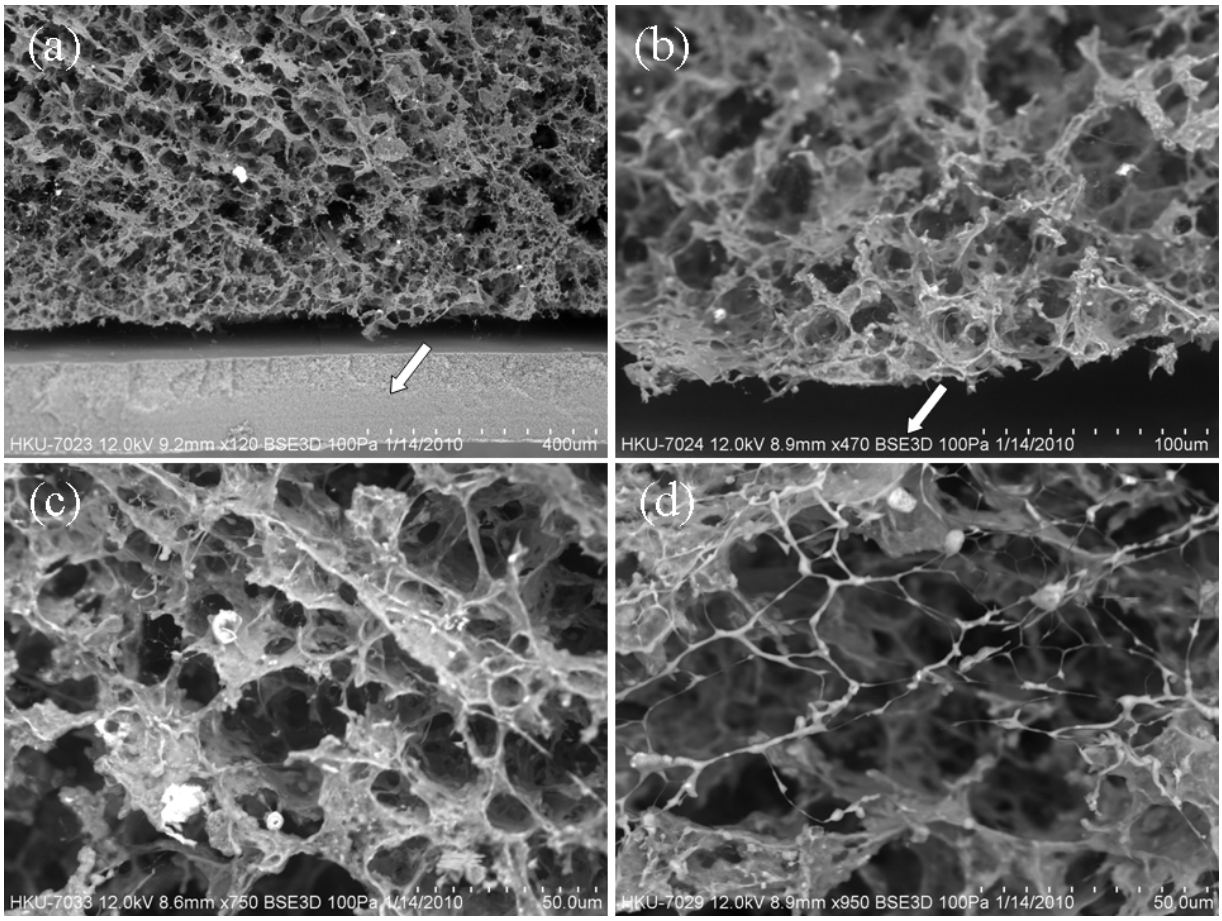

Fig. 2. ESEM images of (a) the cross-section and (b,c,d) detailed structure of the sludge cake formed on a MF membrane filter through direct filtration of the suspended bulk sludge from a MBR. The arrows point to the membrane filter.

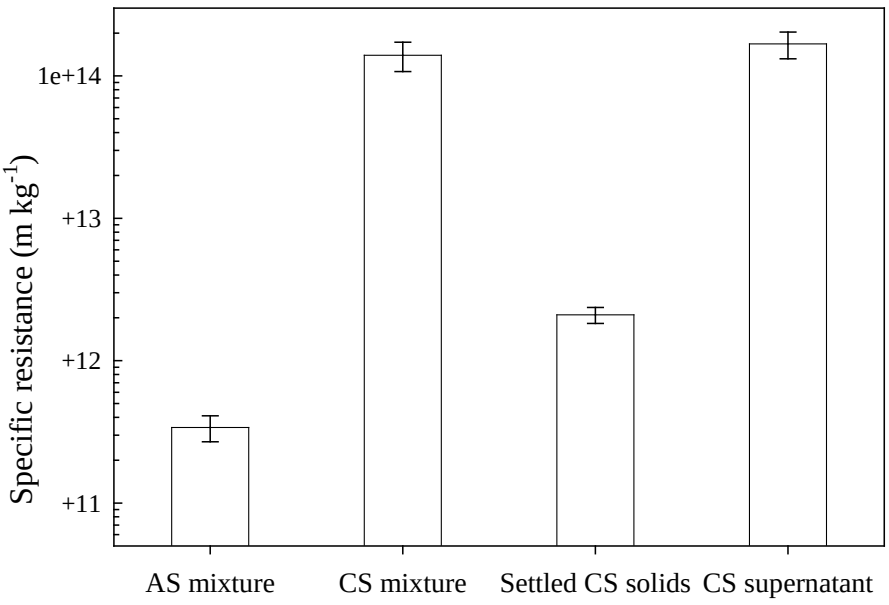

Fig. 3. Comparison of the specific filtration resistance of the cake and gel layers formed during filtration of the MBR bulk sludge (AS mixture), the re-suspended MBR cake sludge (CS mixture), the settled solids of the CS mixture and the CS supernatant after settling.

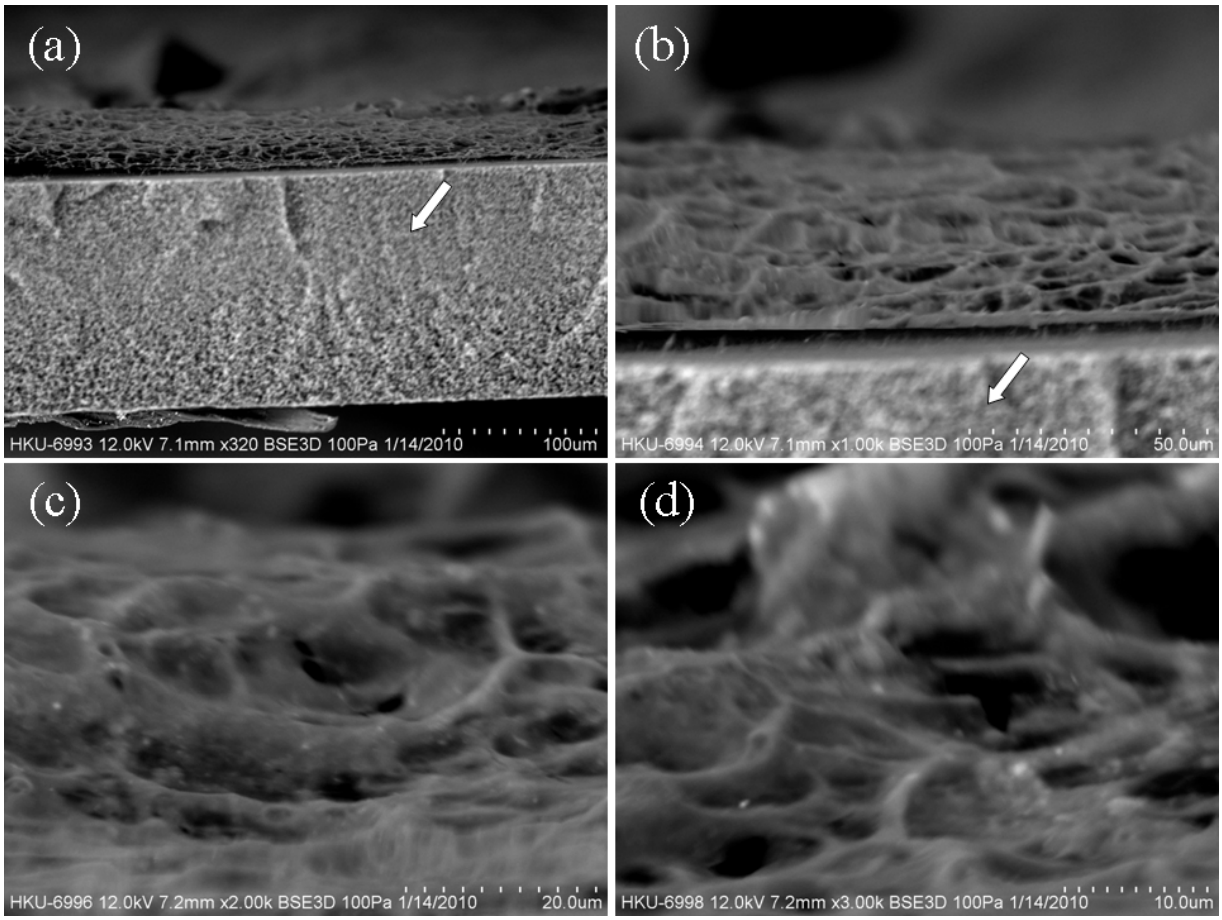

Fig. 4. ESEM images of a layer of BPCs retained on the MF membrane filter through filtration of BPC dispersion, with increasing magnification from (a) to (d). The arrows point to the membrane filter.

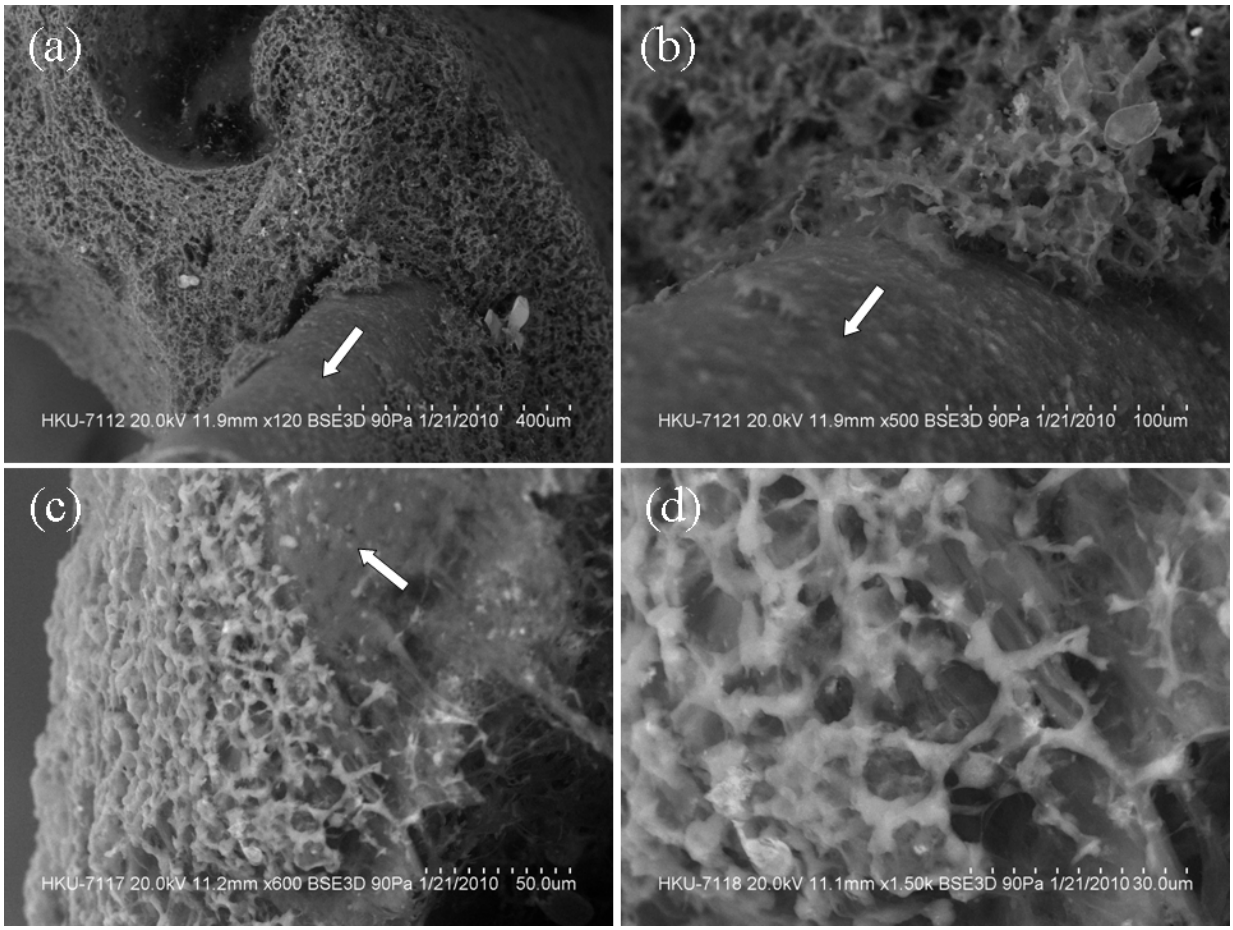

Fig. 5. ESEM images of (a,b) the sludge cake layer deposited on the membrane module in the MBR and (c,d) its bottom BPC layer after removal of the main body of the sludge cake. The arrows point to the hollow-fibre membrane.